Detection of Tidal Stream Turbine Rotor Imbalance Faults for Turbulent Flow Conditions and Optimal Tip Speed Ratio Control

Matthew Allmark*†, Paul Prickett*‡ and Roger Grosvenor*§
*School of Engineering
Cardiff University,The Parade Cardiff, Wales. CF24 3AA
†Allmarkmj1@cardiff.ac.uk
‡Prickett@cardiff.ac.uk
§Grosvenor@cardiff.ac.uk

***Abstract*—The paper presents a methodology for the Condition Monitoring (CM) of tidal stream turbines. The process is based on the use of, so-called, Transient Monitoring Surfaces (TMS) developed by the authors. In this paper the TMSs have been used to detect rotor imbalance faults. To test the use of TMS for CM drive train simulations were undertaken. The simulations undertaken relate to a lab-scale turbine subjected to turbulent flows and an optimal λ control scheme based on Vector Oriented Control (VOC). The simulations are parametrised based on experimental data relating to testing undertaken with varying degrees of rotor imbalance. Use of the TMS gave promising results for the detection of various rotor imbalance conditions. Differing levels of discrepancies between the 'normal operating' or 'baseline' surface were found for differing fault severities. It was also found that a minimum amount of data is required to gain convergence in the surface structure - in this case data sets relating to 5 rotations of the turbine were required to make a suitable fault detection.**

***Index Terms*—Condition Monitoring, Tidal Stream Turbine Rotor Damage, Transient Monitoring Surface, Time Synchronous Averaging, Fault Detection, Hardware-in-the-loop Simulation.**

I. Introduction

Tidal Stream Turbines (TST) are certain to be subjected to harsh marine environments that will impose extreme and cyclic loading scenarios upon turbine sub-assemblies. TST blades in particular are going to experience the full effect of these loading cases. This is known to be causing operational issues linked to reliability concerns including the possibility of early failure [1]. Whilst these loading regimes and associated rotor faults are to a degree unavoidable, the impact of such failures could be reduced with the intelligent monitoring of TST rotors.

A variety of approaches to turbine rotor monitoring have been researched. However, these have normally required the installation of transducers and monitoring systems within the turbine rotor assembly. As with any instrumentation system, the system itself may be subject to reliability issues. To enhance the monitoring functions available for TST applications, Condition Monitoring (CM) approaches based upon the acquisition and analysis of generator signals have been developed [2]. As this approach utilises readily available TST operational data, the approach could have the benefit of not requiring additional sensors, data acquisition systems and data management systems. To date these approaches have been tested primarily during steady-state turbine operation and were based on the characteristics observed within the frequency domain [3].

The paper presents research undertaken considering the application of an alternate algorithmic approach to TST rotor monitoring which utilises parametric surfaces. The specifics of the a parametric surfaces and their construction are detailed in Section II, along with a review of other monitoring approaches currently being researched.

To test the algorithmic approach transient turbine operations were simulated via hardware-in-the-loop simulations utilising back-to-back permanent magnet synchronous machines (PMSMs) as shown in fig 1. This drive train test rig and TST simulation process are briefly outlined along with the method utilised for optimum tip speed ratio (λ) control. The approach utilises a parametric turbine model which captures mean and transient rotor behaviour. The data used to parametrise the model in this case were acquired via flume testing, details of the test campaign can be found in [2].

The input of a variety of stochastic turbulent fluid velocity time series can be applied as required by the specific simulation being enacted. These time series were generated via spectral methods for a length scale of 4 m at a 10% turbulence intensity [4]. The effect of the transient turbine operation, resultant from the interaction of the in-putted fluid velocity time-series and the optimum λ control strategy, on the CM process was considered.

II. Condition Monitoring of Tidal Stream Turbines

A. Literature Review

The improvement and assurance of the reliability of tidal stream turbines and their sub-assemblies must be considered to be a major factor in the realisation of a well-functioning tidal stream energy industry. It has been argued that in order to achieve a levelised cost of energy (LCOE) that is competitive within the market place turbine availability should be above

75% [5]. In moving toward a higher technology readiness level (TRL) and to underpin the significant levels of investment required it has also been stated that the reliability of TSTs and their components must be demonstrated [6] [7]. Experience within the wind energy sector has suggested that online CM and fault detection could minimise maintenance costs and improve availability of the energy extraction technology [8] [9] [10].To inform the development of CM approaches a review of publications addressing the topic has been made. A brief summary is presented herein.

Caselitz et al [11] presented one of the earliest papers aimed specifically at the CM of TSTs. The paper aimed to apply and adapt knowledge acquired in the CM of both on-shore and off-shore wind turbines (WTs). The researchers advocate a system containing many of the elements included in a WT monitoring systems, including accelerometers for gearbox and baring vibration monitoring and fibre bragg gratings for blade and structural load monitoring. The system is supported by environmental measurements, specifically by measurements of the fluid velocity upstream of the turbine rotor. This work goes on to outline the generalities of some CM algorithms to be applied to TSTs based on the hardware set-up outlined.

Sloan et al [12] presented considerations of many of the reliability issues faced by TSTs and the associated monitoring hardware. In [13] Mjit et al conducted work considering order analysis of vibrational data as a means of fault detection, the work was first conducted on a commercial fan and later extended to monitoring of a small boat propeller. The work also discussed elements of the data storage and capture processes. The order analysis methods applied were successful in identification of imbalance and misalignment. The research undertaken and presented by Mjit et al was extended in 2011 [14] to incorporate a more fully developed Smart Vibration Monitoring System (SVMS) which handled much of the data capture storage and processing autonomously. The system included many of the techniques performed off-line by vibration monitoring specialists including advanced signal processing of vibration data. Specifically the software processed raw vibrational data via Power Spectral Density, Fractional Octave, Cepstrum, Hilbert Envelope, Wavelet Transform and overall vibrational statistical characteristics. The process was developed using LabVIEW and tested using a drive train test rig setup to harbour fault conditions by attaching weights to the drive train. Changes to the performance metrics calculated via the advanced signal processing operations listed above were successfully tracked for three differing levels of fault severity and for two rotational velocities. Further works were published by [15], the publication presented an overview of many of the condition monitoring processes as applied by the researchers to the TST drive train simulation apparatus previously developed.

Duhaney et al [16] acquired data from the six accelerometers mounted on a dynamometer setup similar to that used for this study. Data was captured for baseline or normal turbine operation, low fault severity and high fault severity. The data sets were pre-processed to extract time-frequency information via the Haar Wavelet transform, resulting in 18 files of 10,000 readings. Seven machine learning processes (decision tree, Naive Bayes, 5-NN, Logistic Regression, MLP, SVM and random forest) were then applied to the data sets in order to test the ability of the machine learning procedures to make successful fault or no-fault classification. Mixed results were found for the differing machine learning algorithms with the random forest and decision tree classifiers having 100% correct classifications and Nave Bayes, 5-Nearest Neighbour and logistic regression having the highest misclassification rates. Further publications [17] [18] [19] build on the research undertaken by Duhaney et al, the publications present the development of a variety feature extraction and machine learning approaches.

In [20] Waters et al presented research considering the detection, localisation and identification of bearing faults in TST applications. The paper presented models for bearing loading under bearing race cracking. The models were then used to guide the development signal processing methods which were then applied to vibration signals acquired from two accelerometers mounted on dynamometer test beds. The need, requirement and impact of the adoption of CM systems within the TST industry was considered in [21]. The use of TST stanchion thrust measurements for CM of TST blades was reported by Grosvenor et al [22]. This utilised a combination of CFD modelling exercises with flume testing experiments to develop and test a CM approach based on frequency analysis of both computed and measured turbine thrust signals. The work showed that increasing presence of the turbine rotational frequency observed in thrust spectra was a useful indicator of turbine rotor imbalance.

Whilst the number of research publications in the specific area of TST condition monitoring was found to be limited, research in this area has been highlighted as an important aspect of TST development. To support this notion a research project known as TidalSense was setup and funded under a European Commission in 2009, [23]. The project was then extended to become TidalSense Demo in 2011 [24]. The work undertaken by the research project utilised a number of industrial partners and research institutions with the goal developing and demonstrating approaches to the CM of TST. The work focused on the use of Long Range Ultrasonic Technology (LRUT) to inspect cabling and turbine blades [24]. The process of using guided Ultrasonic waves imparted by an actuator with the blade response to the waves recorded by sensors was developed and illustrated over the course of the two projects [25] [26]. The work developed throughout the overall TidalSense project allowed for the imbedding of ultrasonic sensors during composite turbine blade manufacture creating a robust solution.

B. Normalised Parameter Surfaces

The notation of defining a surface of observed torsional amplitudes at harmonics of the turbine rotational velocity over a range of operational λs was initially considered within this research as a modelling device and was presented in [2]. These surfaces were then utilised to develop drive train simulations.

It is shown in [2] that the amplitude at harmonics of the turbine rotational velocity, when normalised by the mean torque value, were in close proximity for various fluid velocities for specific λ values. This notion led to the development of a condition monitoring tool based on the surface construction process.

To utilise such surfaces as a monitoring tool a trending or characterisation process is first required to initially generate a surface relating to normal turbine operation. Then, future operational characteristics can be compared with the trained surface. A comparison process can be utilised to generate alarm conditions and diagnostic reasoning or simply to further characterise the normal turbine operation surface. The difference between the surfaces are captured in this case by the so-called sum of surface error (SOSE). The SOSE indicator is simply the sum of the magnitude of discrepancies between the measured surface and the normal operating surface trended previously. It is noted that for this baseline study a simple approach was considered sufficient - it is, however, advised that more nuanced methods of comparison should be researched.

The process of generating the surfaces uses measured rotor torque, (τ), signals. The general algorithm utilised for the surface generation was:

- Normalise τ Data
- Time Synchronous Averaging (TSA) of τ Data.
- Calculate the spectrum of the TSA process output.
- Add spectrum to surface indexed by rotational velocity harmonics and λ.

The algorithm proposed is dependent on correct normalisation and indexing during surface creation. It was found during the construction of the surfaces that normalising and indexing for surface creation became less defined with increasingly transient turbine operation, for example under high turbulence loading combined with variable speed control. As such developments to the algorithm outlined were made and the resulting surfaces termed, Transient Monitoring Surfaces (TMS).

C. Transient Monitoring Surfaces

The process of generating the TMS follows the same general procedure outlined above; however, under transient turbine operation the mean rotor torque, $\bar{\tau}$, used to normalise the data can become non-stationary and may fluctuate due to the interaction between turbulence within the on-coming fluid velocity and the control scheme utilised. To develop a method for effectively normalising the rotor torque data to allow for the comparison of data recorded under differing fluid velocities and turbine rotational velocities the structure of the turbine rotor model presented in [2] was considered. Generally the structure of the rotor torque model was of the following general form:

$$\tau(t) = \overline{\tau} + \overline{\tau} \cdot A \tag{1}$$

Where A, in the case of the turbine rotor model was a Fourier series representing the fluctuating component of the turbine drive shaft torque. In the current model structure the fluctuating components are related to turbine rotor operation and more specifically to the effect of turbine/stanchion interactions and rotor imbalance. Accordingly the fluctuating components captured in A are explicitly a function of the turbine rotational displacement. They are also implicitly a function of time due to the rotational velocity of the turbine and the effect of the varying fluid velocity and the relationship between the two quantities. This has been captured via scaling of A by the mean torque value,$\overline{\tau}$. In the generation and use of the model until this point, the data sets considered generally adhered to the condition that, $\overline{\tau} = Constant$. This was a simplifying condition which resulted from consideration of steady state turbine operation. However, as the goal of the research presented herein is to consider the effectiveness of the CM approach under non-steady state turbine behaviour, it was consider that, $\overline{\tau} = f(t)$. Whilst the model described in [2] is considerate of the torque developed at the turbine rotor, the CM strategy proposed seeks to utilise readily available generator signals. As such the quadrature axis current, i_q, has been used as analogue for τ, reasoning behind this choice was derived from the standard modelling equations for a PMSM and can be found in [2]. Then equation (1) becomes:

$$i_q(t) = \overline{(i_q)}(t) + \overline{(i_q)}(t) \cdot A \tag{2}$$

It then readily follows that the quadrature axis current observed can be normalised in the following manner to give an estimate of A, which as proposed relates specifically to turbine operational effects:

$$A = \frac{i_q(t) - \overline{(i_q)}(t)}{\overline{(i_q)}(t)} \tag{3}$$

This normalisation method allows for the development of the monitoring surface which relates to relative fluctuation amplitudes that are resultant from the turbine operational characteristics of interest, such as any rotor imbalance and the stanchion shadowing effect. However, in utilising such a method it should be considered that the quantity, $\overline{(i_q)}(t)$ cannot be measured directly and therefore will need to be estimated by some other means. To estimate $\overline{(i_q)}(t)$ it was considered that the mean component of the torque developed by the turbine rotor is proportional to the square of the fluid velocity impacting upon the turbine rotor. This gives:

$$\overline{\tau}(t) \propto \overline{(i_q)}(t) \propto U(t)^2 \tag{4}$$

Furthermore, under set point λ control - as considered in this paper - the fluid velocity is proportional to the turbine rotational velocity. Therefore the proportionality in equation (4) can be expressed as,

$$\overline{i_q}(t) \propto U(t)^2 \propto \omega(t)^2 \tag{5}$$

It follows from the above considerations that the rotational velocity may be useful in normalising the observed generator q-axis current to extract A. This will also further support the building of monitoring surfaces which could be more robust under non-steady state conditions. Lastly, it was considered that the fluctuations in the two quantities are of orders of magnitude apart. As such calculating A in this manner would

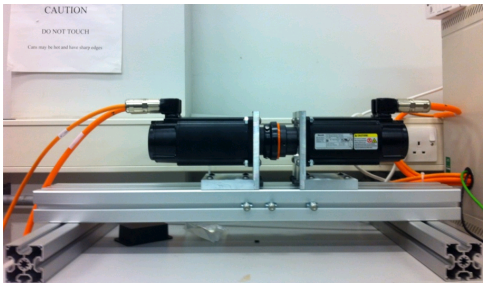

Fig. 1. The drive train test rig which was utilised for scale turbine drive train simulations.

have led to incorrect distortions of the normalised signal and resulting surface. To find the constant of proportionality the ratio of the mean values of the observed quantities was used,

$$c = \frac{mean(\omega(t)^2)}{mean(\overline{i_q}(t))} \tag{6}$$

Finally the normalisation is under taken by:

$$A = \frac{i_q(t) - c \cdot \omega(t)^2}{c \cdot \omega(t)^2} \tag{7}$$

where,

$$\overline{i_q}(t) \approx c \cdot \omega(t)^2 \tag{8}$$

III. Hardware-in-the Loop Simulations

A. Simulation Overview

To fully test the proposed TMS and associated normalisation procedure, simulations were created to represent the effect of both stochastic fluid flow artefacts and differing turbine control processes - simulations relating to optimal λ control are presented in this paper. The general simulation structure is described briefly throughout this section. Fig 2 provides an overview and introduction to the simulation structure. The main observation is that the structure developed allows the appraisal of turbine rotor torque at differing rotor displacements under a wide range of operating conditions. It is set up to use a one-dimensional stochastic fluid velocity model. The dynamic effects of λ based control to maintain optimum power extraction are also included. The structure culminates in the ability to observe and test differing scenarios using a physical, scaled, drive train test rig.

Fig 2 provides a schematic point-of-reference of the simulation approach highlighting the interaction between the various developed models and control procedures. The resource model, presented briefly in Section III-F, provides flow velocity information to the parametric torque model (Section III-C) and to the control actions (presented in Section III-D) to maintain a set-point tip speed ratio. The parametric model parameters are also set in an informed manner drawing on the scale model flume test results which were presented in [2].

B. Tidal Stream Turbine Topology

The turbine simulated is that of the direct-drive permanent magnet synchronous generator type, connected to the grid via back-to-back power converters. A schematic of the setup can be seen in Fig 3. A fully-rated converter setup is shown with the generator side Voltage Source Converter (VSC) utilised for turbine control and the grid-side VSC utilised for control of power flow to the grid [27]. The VSC used are 6 level Insulated-Gate Bipolar Transistors (IGBTs) with gate firing control via pulse width modulation (PWM).

C. Parametric TST Rotor Simulation

The formulations developed and presented in [2] define a parametric turbine rotor torque model, given by:

$$\tau = \bar{\tau} + \sum_{i=1}^{8} \bar{\tau} \cdot a_i \cdot cos(2\pi\theta + \phi_i) + Z \tag{9}$$

where, Z is a normally distributed strictly stationary random process with mean, $\mu = 0$ and standard deviation:

$$\sigma = 0.011\lambda^2 - 0.074\lambda + 0.13 \tag{10}$$

τ is given by:

$$\tau = C_\tau \frac{1}{2} \cdot \rho \cdot \pi r^2 U^2 \tag{11}$$

a_i is the relative amplitude of fluctuations at various harmonics, i to 8 represented as a surface. ϕ_i is the phase angle at various harmonics, i to 8 represented as a surface. lastly, θ represents the turbine rotational displacement.

D. Optimal λ Control

To simulate turbine dynamics in a representative manner variable speed, optimal λ, turbine control was utilised for the experimental simulations. This was included to allow for adequate appraisal of CM hypotheses based on the simulation results. The method involved taking fluid velocity and turbine rotational velocity measurements required to define the turbine operating tip speed ratio. The measured operating point is compared with a set-point λ value, known prior to operation to give maximum power output under continuous turbine operation. The error value is passed to a controller to regulate the generator load to achieve the torque required to minimise the tip speed ratio error. Fig 4 shows the control diagram for the optimal tip speed ratio tracking control system used during the experimental simulations [28]. It can be seen that the essential element in controlling the generator feedback torque and hence rotational velocity is controlling the load power output via the power converter apparatus. During the experimental simulations the torque set point command was input to the motor drive used and the internal control structure was used which is outlined below.

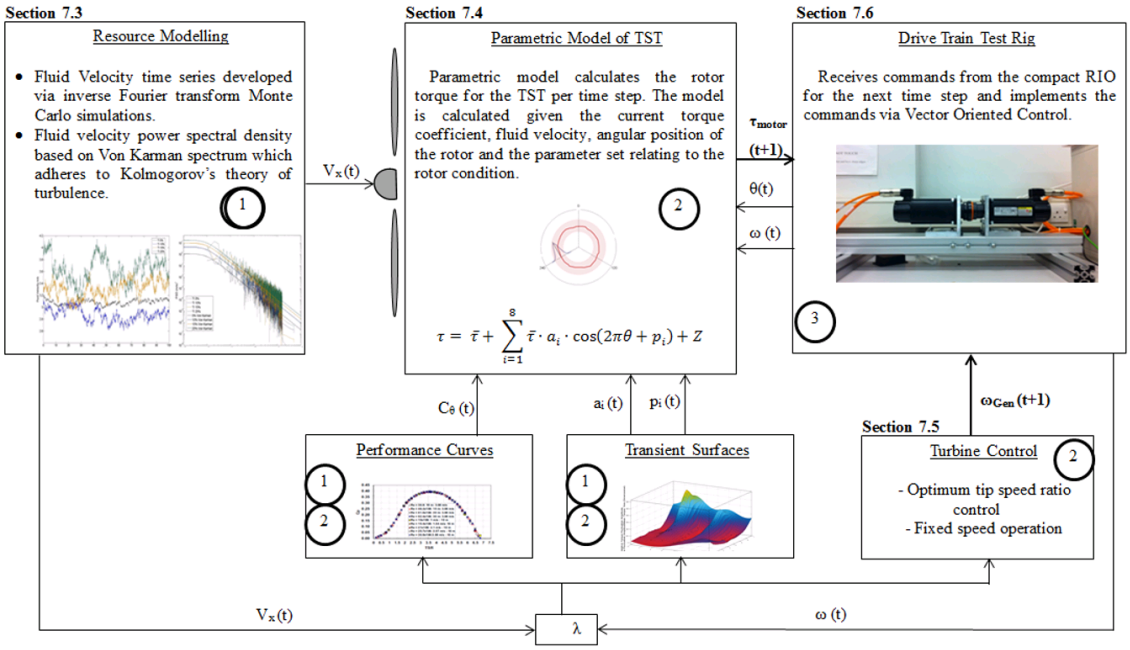

Fig. 2. Schematic of the simulation process utilised in generating turbine simulations and scaled drive shaft emulator testing. The figure shows the 1/20th scale testing results as an input to the parametric rotor model along with the input of a resource simulation model.

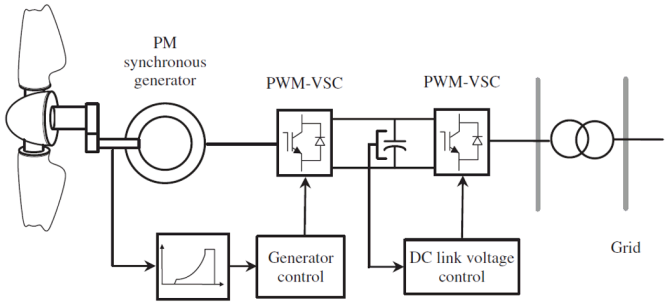

Fig. 3. Schematic of the TST topology represented throughout out the work presented. The figure shows a grid connected direct drive turbine with a Permanent Magnet Synchronous Generator (PMSG). A full-rated convert setup is also shown with the grid side VSC utilised for turbine control and the grid-side VSC utilised for control of power flow to the grid [27].

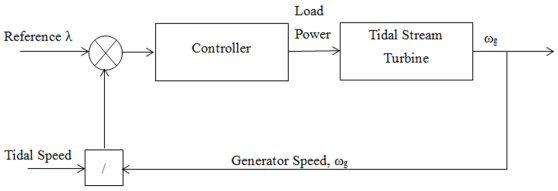

Fig. 4. An example of optimal λ control scheme. Adapted from [28].

E. Vector Oriented Control

The PMSMs utilised for the test rig setup were setup to implement vector oriented control (VOC). In the case of the motor the goal of the VOC was to operate the motor in a similar fashion to a TST via the application of appropriate torsional loads which are calculated via the outlined rotor model. The goal of the VOC for the generator is to control the generator load in order to realise optimal λ control. The idea of vector oriented control has been previously utilised for motor and generator control. Its use in relation to tidal stream turbine control has been reported [29]. The process related to applying this to wind turbine control has also been reported [27]. In the case of a PMSG, this is done by noting that under normal operation the i_d current in the torsion equation for a PMSG is weakening the magnetic flux producing the generator feedback torque. The i_d can therefore be set to zero to give optimum torsional performance, this gives:

$$\tau_e = \frac{2}{3} \cdot p \cdot \psi \cdot i_q \tag{12}$$

For a set-point torque required to accelerate or decelerate the turbine velocity to the required optimal rotational velocity the reference direct and quadrature currents are given by:

$$i_{dref} = 0 \tag{13}$$

$$i_{qref} = \frac{3}{2} \frac{T_{sp}}{p \cdot \psi} \tag{14}$$

The required voltage in the direct and quadrature axis can be found be re-arranging:

$$v_{dref} = Ri_d + \omega_r L_q i_q \tag{15}$$

$$v_{qref} = -Ri_q - \omega_r L_d i_d \omega_r \psi \tag{16}$$

The voltage reference signal is then input into a PWM module which generates the switching sequence for the IGBT to regulate the phase voltages of the generator to give the required generator feedback torque which will result in the set-point λ

value required for peak power extraction. The VOC control scheme was implemented in the drive systems of the PMSMs and was developed by Bosch Rexroth as a standard control system for the machines utilized.

F. Fluid Velocity Simulation

The simulations outlined in this paper use the simplification that the turbine would be subjected to plug flow (non-profile flow) conditions. This simplification was necessary as this was the approximate flow conditions observed during the flume testing campaign used to gather data for the model parametrisation. The plug flow assumption leads to a convenient representation of the flow conditions hitting the turbine rotor. The flow is represented by:

$$U_x(t) = \bar{U_x} + u'_x(t) \tag{17}$$

where $U_x(t)$ is the fluid velocity at time t decomposed into a stationary mean fluid velocity $\bar{U_x}$ and a fluctuating component $u'_x(t)$ which is time varying with the x direction perpendicular to the turbine rotor plane. A natural model for representing the fluid flow given by the above is to model the fluid velocity fluctuations as a stationary process with given power spectral density characteristics. Furthermore utilising Kolomogrovs theory of turbulence the amplitude of the power spectrum should be proportional to $f^{-5/3}$ as $f \to \infty$. The Von Karman spectrum, as utilised by previous investigators [4] for reliability simulations adheres to the above condition and can be written in the non-dimensional form:

$$\frac{fS_u(f)}{\sigma_u^2} = \frac{\frac{4fL}{\bar{U_x}}}{[1 + 70.79(\frac{fL}{\bar{U_x}})^2]^{\frac{5}{6}}} \tag{18}$$

where $Su(f)$ is the spectral density function for the process, L is the length scale, σ_u is the standard deviation of the process $u_x(t)$. In the above the x subscript has been omitted for brevity as the formulation outlined relates to a one-dimensional simulation.

IV. Results

A. Simulation Campaign Overview

In order to test the proposed CM method using TMSs, hardware-in-the-loop simulations were undertaken utilising the form presented above using model parametrisations derived via flume testing of a $1/20^{th}$ scale model TST. The scale model was set up to harbour known sub-optimal rotor conditions. A full description of the flume testing procedure followed can be found in [2]. Four levels of rotor imbalance conditions were tested at a three differing fluid velocities (0.9 m/s, 1.0 m/s and 1.1 m/s). The rotor imbalance levels were achieved by setting the pitch angle of differing blades away from the optimum for the turbine rotor. For the 3-bladed rotor, housing adapted Wortman FX 63-137 blades, the optimal pitch setting was found to be 6^o as reported in [30]. The cases tested during flume testing were:

Case 0→ Blade 1: 6^o, Blade 2: 6^o, Blade 3: 6^o.
Case 1→ Blade 1: 9^o, Blade 2: 6^o, Blade 3: 6^o.
Case 2→ Blade 1: 12^o, Blade 2: 6^o, Blade 3: 6^o.
Case 3→ Blade 1: 6^o, Blade 2: 12^o, Blade 3: 9^o.

The simulations were created for approximately 90 seconds, for a mean fluid velocity of 1 m/s and a turbulence intensity of 10 $\%$. The length scale associated with the turbulence was set to 2 m and as discussed variable speed, optimal λ control was executed. Initially simulations were undertaken for the optimal rotor setting at three differing λ values (3.0, 3.6 and 4.2) - these simulations were used to create the benchmark surface shown in Fig 9. Rotor imbalance simulations were then undertaken for the three fault cases (as well as an additional optimum case as a control study) and a single set-point λ value of 3.6 (peak power for the simulated turbine). The surfaces generated via the four remaining simulations were then compared with the baseline.

B. Simulation Results Overview

Fig 5 shows the results of non-steady state simulations with the inclusion of the turbulent fluid velocity time series discussed. It can be seen that fluid velocity fluctuations are included in the simulations and as a result of the optimal λ control scheme adopted, rotational velocity fluctuations of the turbine can also be seen. Furthermore due to the change in fluid velocity additional fluctuations can be seen in the torsional input of the motor simulating the turbine input to the drive system. These additional fluctuations are also evident in traces for power output and quadrature axis current measured via the generator PMSM control system.

C. Transient Monitoring Surface Results

Fig 6 shows the effect of normalising the generator q-axis current data on the TSA process used to construct the output monitoring surfaces. The figure shows the deviation of the recorded data from the TSA characteristic with increasing numbers of rotations included in the TSA process. The figure shows that normalising the generator output data as described results in better convergence to an underlying TSA characteristic. It can be seen that minimal convergence to an underlying TSA process was observed for the non-normalised simulation data. Furthermore the figure also shows greater deviation from the calculated TSA characteristics for the higher tip-speed ratio values. Figs7 to 9 show the stages in generating the baseline TMS. Fig 7 shows graphically the TSA process as undertaken - the darker line highlights the mean trace with the raw data shown as thinner lines. The spectrum plots for each TSA mean trace are then shown in 8 - with the frequency axis scaled to give harmonics of the rotational frequency of the turbine. It can be seen that a distortions in the spectrum were found for differing λ values with prominent harmonics oberved at 1^{st}, 3^{rd} and 6^{th} harmonics. These spectrum are combined to create the characteristic surface shown in fig 9.

D. Fault Detection and Diagnosis

Fig 10 shows the SOSE error observed for each simulation case as more rotations are included in the data sets used to create the surfaces. Initially, before approximately 5 rotations

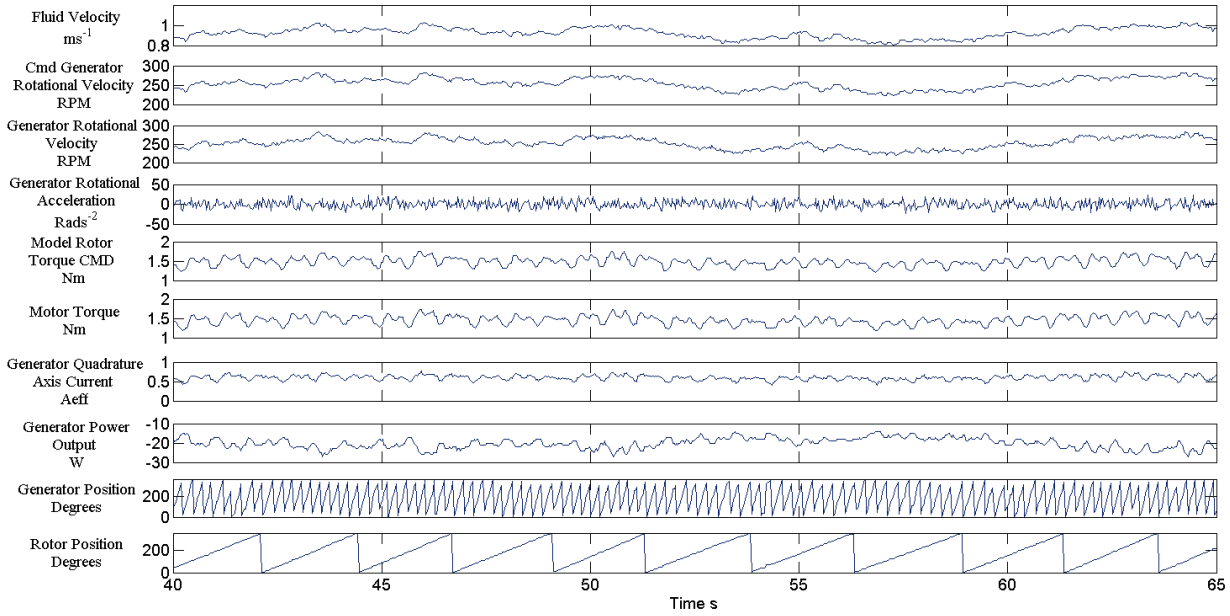

Fig. 5. Results from the real-time drive train simulations, the case shown is the optimum rotor case with TI = 0.1 with optimal λ control utilised

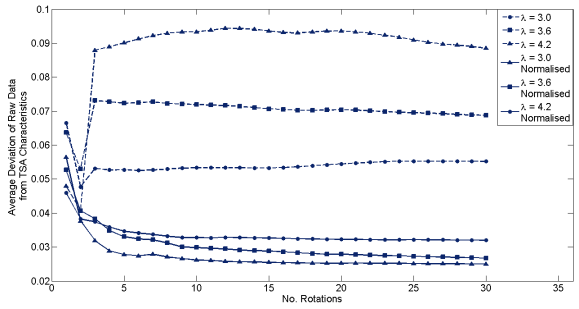

Fig. 6. Deviation of the generator quadrature axis datasets form the TSA means characteristics for normalised and non- normalised datasets and various λ values.

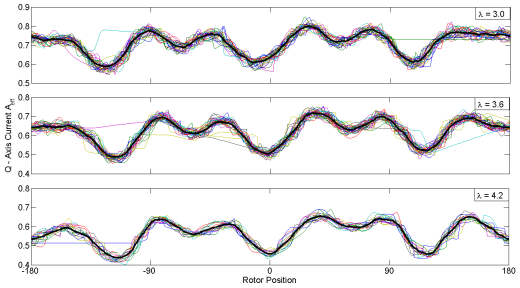

Fig. 7. Graphical view of TSA process used to create the normal operation TMS.

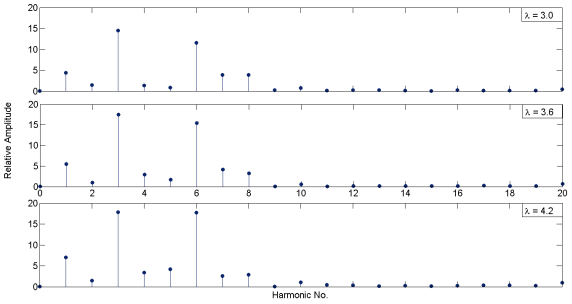

Fig. 8. Spectrum generated to be inserted into the TMS for normal turbine operation.

are included in the surface generation process, the sum of surface error measurement is relatively large for all cases. As more rotations are included in the surface generation process the sum of surface error measurement reduces in all cases. This indicates that the turbine is more accurately characterised by increasing amounts of data. As more data is included in the surface construction the figure shows that sum of surface error starts to converge to a given value for each fault condition. The two blade offset condition sum of surface error measurement is the lowest of the fault conditions, this followed by the 3^o offset case with the largest sum of surface error observed for the 6^o offset case. Fig 10 also shows that second optimum simulation yielded the lowest sum of surface error.

V. Discussion

The process of creating characteristic surfaces for the steady-state test scenarios was developed, via inclusion of further normalisation processes, to include non-steady state turbine operating scenarios. In terms of the optimal λ control scenarios the TMS generation process was undertaken via a novel normalisation process as applied to the measured generator quadrature axis current. The normalisation process made use of the proportionality between observed drive shaft torque and the square of the rotor velocity as imposed by the optimal λ control strategy. In this way data segments

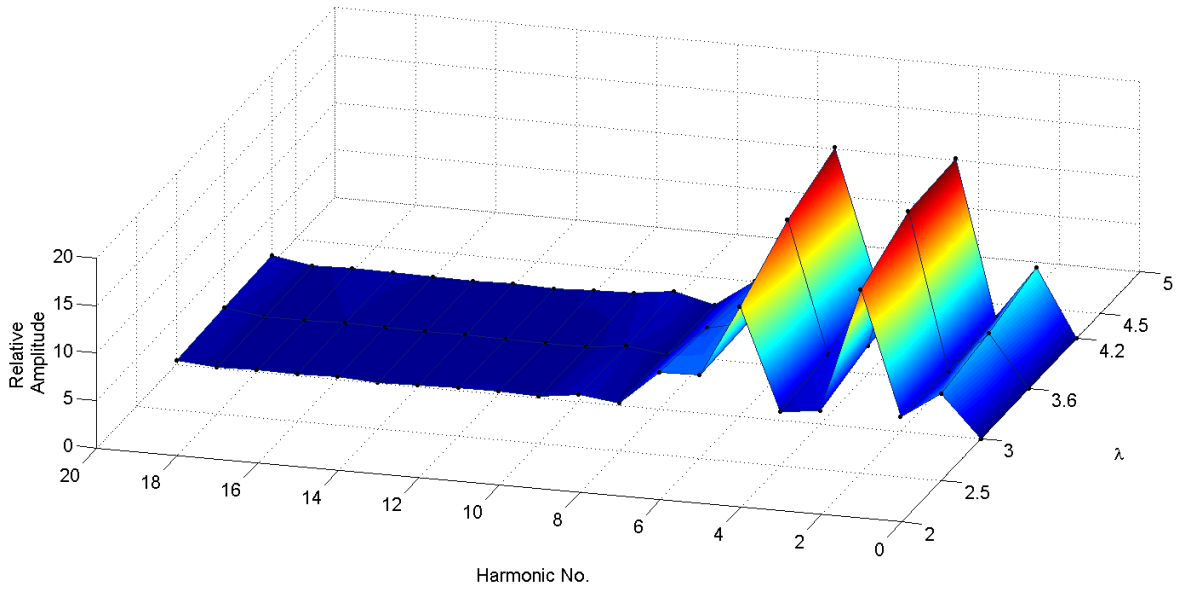

Fig. 9. TMS generated for normal turbine operating conditions. This surface represents the non-fault condition benchmark.

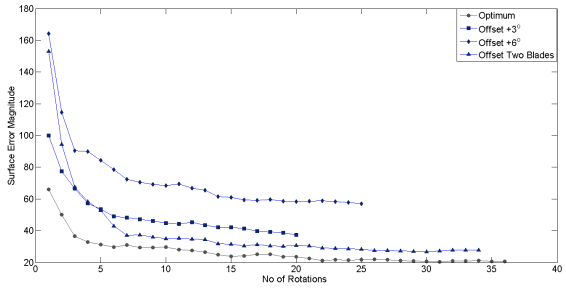

Fig. 10. Development of the Sum of Surface error value observed for differing rotor conditions plotted against the number of rotations included in the surface generation process.

fed into the TSA process required to create the monitoring surfaces could be normalised to compare the TSA outputs for a given λ value at differing fluid velocities and turbine rotational velocities. This was considered to be a strong aspect of the monitoring surface technique as applied to the optimal λ control scheme data sets. Developing the TMS generation process to a condition monitoring procedure was undertaken by considering the distortion of the monitoring surfaces under anomalous rotor conditions relative to the generated surface for optimal rotor conditions. This was achieved by considering the SOSE between the surfaces generated under anomalous conditions and optimal conditions. It was found that varying fault conditions gave varying sum of surface error values. Also it was found that as greater numbers of rotations were utilised in constructing the surfaces for each differing condition the sum of surface error relative to the normal operating surface seemed to converge to a given value. This was considered to potentially provide stability and avoid false alarms when generating detection and diagnostic reasoning based on the approach. The relative success and stability of the method in spite of fluctuating fluid velocities and rotational velocities was seen as a significant result. This result indicates that the method utilised was sound when faced with non-steady state turbine operation and optimal λ turbine control. Another aspect of the process that was seen as an asset was that the method didnt rely on fluid velocity measurements in order to construct the normalised monitoring surfaces. This was considered to allow for the application of the method to a variety of optimal λ turbine control schemes, such as hill climb and optimal torque turbine control. Lastly, the researchers note that this process has been illustrated and tested with minimal volumes of data. In-terms of the application of the process to full-scale turbine deployments, the trending period used to create the baseline surface will by necessity have to be sufficient to allow for reasonable surface interpolation and information extraction. More localised SOSE measurements can then be utilised for more robust monitoring.

VI. Conclusions

A set of approaches to turbine transient characterisation, based on the development of TMSs, were applied to the non-steady state data. The approaches were data intensive and gave promising but non-conclusive results. Further testing these processes is required to understand if the normalisation and characteristic surface generation process are effective. However, the results observed gave varying levels of SOSE for differing rotor anomalies which could facilitate both fault diagnosis and detection. This notion was further posited by the convergence of the SOSE value for each fault to a single value.

VII. Further Work

The use of the TMS should be tested further at the conditions outlined to gain further insight into their application. Lastly, the discretization of the harmonic index of the TMS surface could be increased subject to greater volumes of data. Likewise the range of harmonics captured by the surfaces could be increased. This would allow for the study of the usefulness of the TMS to detect other drive train faults.

Acknowledgements

The authors would like to thank industrial collaborators Bosch Rexroth and National Instruments. This work was funded via EPSRC as part of the SUPERGEN UKCMER Grand Challenge project.

References

[1] T. M. Delrom, "Tidal stream devices: Reliability prediction models during their conceptual and development phases," Ph.D. dissertation, Durham University, 2014.

[2] M. J. Allmark, "Condition monitoring and fault diagnosis of tidal stream turbines subjected to rotor imbalance faults," Ph.D. dissertation, Cardiff University, 2017.

[3] M. J. Allmark, C. Frost, R. I. Grosvenor, and P. Prickett, "Time-frequency analysis of tst drive shaft torque for tst blade fault diagnosis." in *Eleventh European Wave and Tidal Energy Conference*, Nantes, France, 2015.

[4] D. V. Val, L. Chernin, and D. V. Yurchenko, "Reliability analysis of rotor blades of tidal stream turbines," *Reliability Engineering and System Safety*, vol. 121, no. 1, pp. 26–33, 2014.

[5] D. Magagna, A. MacGillivray, H. Jeffrey, C. Hanmer, A. Raventos, A. Badcock-Broe, and E. Tzimas, "Wave and Tidal Energy Strategic Technology Agenda," SI Ocean, Tech. Rep., 2014. [Online]. Available: http://www.oceanenergy-europe.eu/images/OEF/140215_SI_Ocean_-_Srategic_Technology_Agenda.pdf

[6] J. Wolfram, "On Assessing the Reliability and Availability of Marine Energy Converters: The Problems of a New Technology," *Proceedings of the Institution of Mechanical Engineers, Part O: Journal of Risk and Reliability*, vol. 220, no. 1, pp. 55–68, jan 2006. [Online]. Available: http://sdj.sagepub.com/lookup/10.1243/1748006XJRR7

[7] S. Weller, P. Thies, T. Gordelier, and L. Johanning, "Reducing Reliability Uncertainties for Marine Renewable Energy," *Journal of Marine Science and Engineering*, vol. 3, no. 4, pp. 1349–1361, nov 2015. [Online]. Available: http://www.mdpi.com/2077-1312/3/4/1349/

[8] Z. Hameed, S. H. Ahn, and Y. M. Cho, "Practical aspects of a condition monitoring system for a wind turbine with emphasis on its design, system architecture, testing and installation," *Renewable Energy*, vol. 35, pp. 879–894, 2009. [Online]. Available: http://ac.els-cdn.com/S0960148109004704/1-s2.0-S0960148109004704-main.pdf?_tid=3a081722-1e87-11e7-8ba2-00000aacb35f&acdnat=1491895360_6cc5a6e2ecca741e5ddcfab8764090a7

[9] W. Yang, P. J. Tavner, C. J. Crabtree, and M. Wilkinson, "Cost-Effective Condition Monitoring for Wind Turbines," *Industrial Electronics, IEEE Transactions on*, vol. 57, no. 1, pp. 263 –271, jan 2010.

[10] Z. Tian, T. Jin, B. Wu, and F. Ding, "Condition based maintenance optimization for wind power generation systems under continuous monitoring," *Renewable Energy*, vol. 36, no. 5, pp. 1502–1509, may 2011.

[11] P. Caselitz and J. Giebhardt, "Condition monitoring and fault prediction for marine current turbines," in *International Conference Ocean Energy; from Innovation to Industry*, 2005, pp. 1–8.

[12] J. C. Sloan, T. M. Khoshgoftaar, P.-P. Beaujean, and F. Driscoll, "OCEAN TURBINES A RELIABILITY ASSESSMENT," *International Journal of Reliability, Quality and Safety Engineering*, vol. 16, no. 05, pp. 413–433, oct 2009.

[13] M. Mjit, P.-P. J. Beaujean, and D. J. Vendittis, "Fault Detection and Diagnostics in an Ocean Turbine Using Vibration Analysis," in *Volume 8: Dynamic Systems and Control, Parts A and B*. ASME, 2010, pp. 535–543. [Online]. Available: http://proceedings.asmedigitalcollection.asme.org/proceeding.aspx?articleid=1616638

[14] M. Mjit, P.-P. J. Beaujean, and D. j. Vendittis, "Smart Vibration Monitoring System for an Ocean Turbine," in *2011 IEEE 13th International Symposium on High-Assurance Systems Engineering*. IEEE, nov 2011, pp. 252–260. [Online]. Available: http://ieeexplore.ieee.org/document/6113905/

[15] ——, "Comparison of Fault Detection Techniques for an Ocean Turbine — PHM Society," in *Annual Conference of the Prognostics and Health Management Society 2011*, Quebec, 2011. [Online]. Available: https://www.phmsociety.org/node/625

[16] J. Duhaney, T. Khoshgoftaar, and J. Sloan, "Feature Level Sensor Fusion for Improved Fault Detection in MCM Systems for Ocean Turbines." in *Proceedings of the Twenty-Fourth International Florida Artificial Intelligence Research Society Conference, May 18-20, 2011, Palm Beach, Florida, USA*. Palm Beach: FAIRS, 2011.

[17] J. Duhaney, T. M. Khoshgoftaar, and J. C. Sloan, "Feature Selection on Dynamometer Data for Reliability Analysis," in *2011 IEEE 23rd International Conference on Tools with Artificial Intelligence*. IEEE, nov 2011, pp. 1012–1019. [Online]. Available: http://ieeexplore.ieee.org/document/6103464/

[18] J. Duhaney, T. M. Khoshgoftaar, and A. Napolitano, "Studying the Effect of Class Imbalance in Ocean Turbine Fault Data on Reliable State Detection," in *2012 11th International Conference on Machine Learning and Applications*. IEEE, dec 2012, pp. 268–275. [Online]. Available: http://ieeexplore.ieee.org/document/6406674/

[19] J. Duhaney and T. M. Khoshgoftaar, "Proceedings / 19th ISSAT International Conference on Reliability and Quality in Design, August 5-7, 2013, Honululu, Hawaii, U.S.A." in *19th ISSAT International Conference on Reliability and Quality in Design August 5-7, 2013 - Honolulu, Hawaii, U.S.A.* Honolulu: ISSAT, 2013, pp. 240–244. [Online]. Available: https://issatconferences.org/Content19/19112.html

[20] N. Waters, P.-P. Beaujean, and D. Vendittis, "Targeting Faulty Bearings for an Ocean Turbine Dynamometer — PHM Society," *International Journal of Prognostic Health Management*, vol. 4, no. 021, 2013. [Online]. Available: http://www.phmsociety.org/node/978

[21] F. ELASHA and J. A. TEIXEIRA, "Condition Monitoring Philosophy for Tidal Turbines," *International Journal of Performability Engineering*, vol. 10, no. 5, p. 521, 2014. [Online]. Available: https://www.researchgate.net/profile/Faris_Elasha/publication/263648618_Condition_Monitoring_Philosophy_for_Tidal_Turbines/links/5538b4e20cf2239f4e79b26b.pdf

[22] R. I. Grosvenor, P. W. Prickett, C. Frost, and M. Allmark, "Performance and Condition Monitoring of Tidal Stream Turbines — PHM Society," in *Second European Conference of the Prognostics and Health Management Society 2014*. Nantes: PHM Society, 2014. [Online]. Available: http://www.phmsociety.org/node/1235/

[23] "European Commission : CORDIS : Projects & Results Service : Demonstration of a Condition Monitoring System for Tidal Stream Generators. Tidal Sense." [Online]. Available: http://cordis.europa.eu/project/rcn/102179_en.html

[24] "European Commission : CORDIS : Projects & Results Service : Development of a condition monitoring system for tidal stream generator structures. TidalSenseDemo." [Online]. Available: http://cordis.europa.eu/project/rcn/107809_en.html

[25] K. Makaya, K. Burnham, and C. Campos, "Assessment of defects in wind and tidal turbine blades using guide waves. Engineering Structural Integrity Assessment: from plant and structural design, manufacture to disposal." in *EMAS 2011*. Manchester: EMAS, 2011.

[26] "TidalSense." [Online]. Available: http://www.tidalsense.com/

[27] O. Anaya-Lara, N. Jenkins, J. Ekanayake, P. Cartwright, and M. Hughes, *Wind energy generation : modelling and control*. John Wiley & Sons, 2009.

[28] M. A. Abdullah, A. H. M. Yatim, C. W. Tan, and R. Saidur, "A review of maximum power point tracking algorithms for wind energy systems," *Renewable and Sustainable Energy Reviews*, vol. 16, no. 5, pp. 3220–3227, jun 2012.

[29] B. Whitby and J. Liang, "Field Oriented Control of a Permanent Magnet Synchronous Generator for use in a Variable Speed Tidal Stream Turbine," in *Universities' Power Engineering Conference (UPEC), Proceedings of 2011 46th International*, 2011, pp. 1–6.

[30] A. Mason-Jones, "Performance assessment of a Horizontal Axis Tidal Turbine in a high velocity shear environment." phd, Cardiff University, 2010. [Online]. Available: http://orca.cf.ac.uk/54910/